Int. J. Electrochem. Sci., 15 **(2020)** 9940 – 9947, doi: 10.20964/2020.10.64

International Journal of
ELECTROCHEMICAL
SCIENCE
www.electrochemsci.org

Short Communication

Prediction of Mn Contents of Amorphous Co–Mn Thin Films Formed during Electrodeposition

M. Saitou

University of the Ryukyus, Department of Mechanical Systems Engineering, 1 Senbaru Nishihara-cho Okinawa, 903-0213, Japan.
E-mail: saitou@tec.u-ryukyu.ac.jp

Received: 10 July 2020 / *Accepted:* 5 August 2020 / *Published:* 31 August 2020

The Mn content and crystallographic structure of Co–Mn thin films electrodeposited by rectangular pulse voltages over a megahertz frequency range were investigated using energy dispersive X-ray (EDX) microanalysis and X-ray diffraction (XRD). The EDX analyses demonstrated that in accordance with the phenomenological theory of multi-component electrodeposition (*Int. J. Electrochem. Sci.*, 15 (2020) 6561), the Mn content increased with the cathode potentials, significantly changed at resonant frequencies when the cathode potential was equal to the Mn^{2+} potential barrier, and approached a saturated value. The potential barriers of Co^{2+} and Mn^{2+} were determined to be 1.32 and 2.26 V, respectively. The Co–Mn films containing 40-56 wt% Mn were produced from a Co^{2+}/Mn^{2+} solution with a mole ratio of 1.2. The XRD analysis revealed that the Co–Mn thin films had amorphous structures.

Keywords: amorphous Co–Mn thin film; cathode potential; potential barrier; electrodeposition

1. INTRODUCTION

Co–Mn thin films have attracted research interest because of their wide application in cathode interconnects for solid oxide fuel cells [1-3], super-capacitors [4], magneto-optical recording media [5], catalysts [6] and corrosion resistance [7].

The physical properties of Co–Mn thin films greatly depend on their Mn contents. For successful formation of half metals such as Co_2MnSn, the element contents should have proper stoichiometric ratios. Electrodeposition is an attractive method for fabricating thin films. However, no phenomenological theory to predict the element contents of electrodeposits formed from multi-component solutions has yet been developed. Hence, the effects of electrochemical parameters on the element contents of multi-component electrodeposits have been experimentally investigated [8]. Recently, a phenomenological theory that predicts element contents of multi-component electrodeposits obtained using a MHz frequency pulse voltage was proposed [9]. According to this theory, the element contents are determined

by their cathode potential, potential barriers, and frequencies. In particular, when the potential barrier is equal to the cathode potential, the element contents significantly change at resonant frequencies. The present study demonstrates that the Mn contents of Co–Mn thin films obey the phenomenological theory.

The Co–Mn phase diagram at room temperature [10] shows that Co–Mn thin films have a hexagonal close-packed (HCP) Co phase at Mn content <4 wt%, coexisting phases comprising an HCP Co and β-Mn phase when the Mn content range is 4-50 wt%, and β–Mn phase at the Mn content >50 wt%. Electrodeposited Co–Mn thin films with a low content Mn have the HCP Co phase [8]. However, the phases of electrodeposited materials often deviate from those predicted using thermal equilibrium phase diagrams. In the present study, the crystallographic structures of Co–Mn thin films were shown to have amorphous structures different from those predicted based on the Co–Mn phase diagram.

The aims of the present study are to show that the Mn content of Co–Mn thin films obey the phenomenological theory and that the Co–Mn thin films have amorphous structures.

2. EXPERIMENTAL SETUP

An aqueous solution containing the following chemical compounds was prepared: $CoSO_4 \cdot 7H_2O$ (0.515 mol L^{-1}), $MnSO_4 \cdot 5H_2O$ (0.43 mol L^{-1}), and $KNaC_4H_4O_6 \cdot 4H_2O$ (0.65 mol L^{-1}). Thus, a Co^{2+}/Mn^{2+} solution with a mole ratio of 1.2 was prepared.

A 30 ×10 mm^2 copper plate and a 50 × 40 mm^2 carbon plate were used as the cathode and anode. One side of the copper plate was electrically insulated so as to be deposited only on the other side. The two electrodes cleaned by a wet process were placed parallel to each other in an electrochemical cell filled with the aqueous solution. The solution was kept at 300 K during electrodeposition.

Co–Mn thin films were electrodeposited on the copper plate immersed to a depth of 15 mm in the solution. As the area of the carbon electrode was approximately 27 times larger than the deposited area of the copper plate, the impedance of an electric double layer in series with the carbon electrode in the solution can be neglected. The impedance between the cathode and anode can also be ignored because of the concentrated solution.

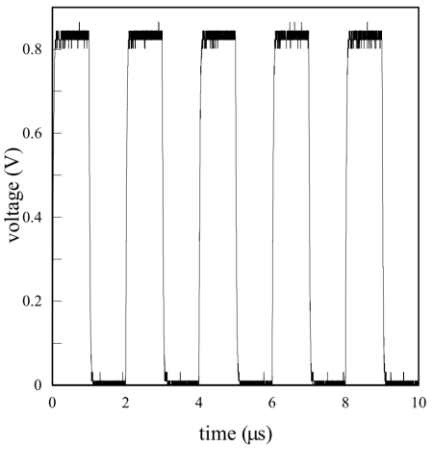

Figure 1. Voltage drops measured between the 22 Ω resistor when a rectangular pulse voltage with an amplitude of 3 V and a frequency of 0.5 MHz was applied to the cell.

The rectangular pulse voltage in a frequency range of 0.4–1.2 MHz was supplied to the cell by a function generator. A 22 Ω metal film resistor was connected in series with the electrochemical cell to measure the current flowing to the cell. The impedance of the metal film resistor was independent of the frequency under 80 MHz. The rectangular pulse current carried in the electrochemical cell was calculated from the voltage drop across the metal film resistor, which was measured with a digital storage oscilloscope.

Figure 1 shows a typical rectangular pulse voltage measured between the metal film resistor when a rectangular pulse voltage with an amplitude of 3 V and a frequency of 0.5 MHz was applied to the cell. As the mean amplitude was 0.82 V in Fig. 1, the cathode potential was calculated as 2.18 V.

After deposition, the Co–Mn thin film electrodeposited on the copper plate was rinsed with distilled water and dried in a vacuum chamber. The Co–Mn thin film was weighed to a precision of 0.1 mg with an electric balance to calculate its film thickness.

The Mn and Co contents of Co–Mn thin films on the copper plate were investigated using energy dispersive X-ray (EDX) microanalysis (Hitachi TM3030). The crystallographic structure of Co–Mn thin films was determined through X-ray diffraction (XRD) (Rigaku Ultima) using CuKα radiation with monochromators of carbon.

3. RESULTS AND DISCUSSION

3.1 Mn content predicted by the phenomenological theory

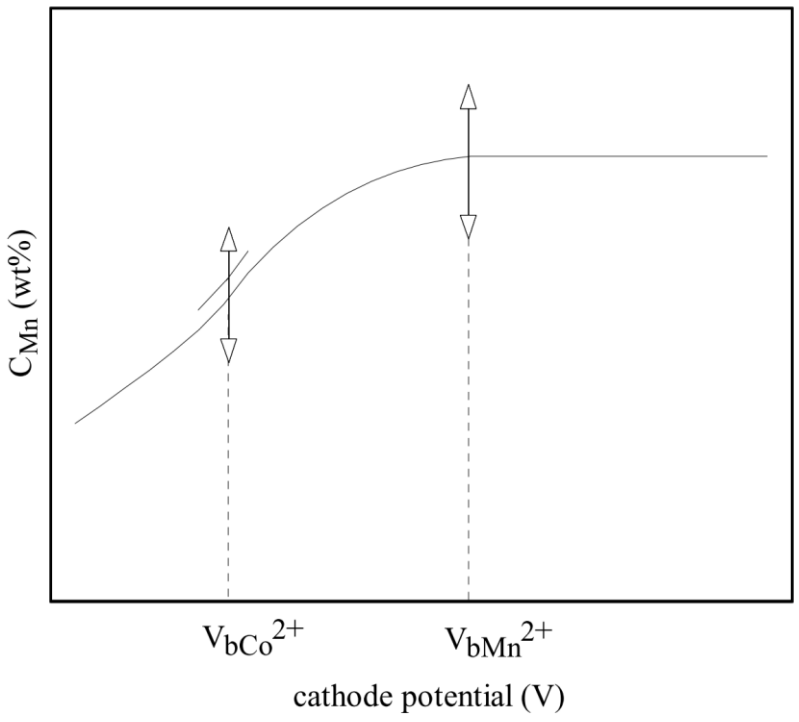

Figure 2. Typical Ni content diagram of Co–Mn thin films assuming $V_{bMn}^{2+} > V_{bCo}^{2+}$.

A phenomenological theory for predicting the element contents of multi-component electrodeposits has already been proposed [9]. In this study, this phenomenological theory is applied to the Mn content of Co–Mn thin films: (1) when the cathode potential, V_c increases to reach the Co^{2+} or Mn^{2+} potential barriers, $V_{bCo}{}^{2+}$ or $V_{bMn}{}^{2+}$, the number of electrons at the Fermi level in the cathode that can pass through the electric double layer owing to the tunneling effect [9] described by the Fowler–Nordheim equation [11] increases. Some Mn^{2+} and Co^{2+} ions change into Mn and Co atoms on the cathode. (2) When $V_c = V_{bCo}{}^{2+}$ or $V_{bMn}{}^{2+}$, the Co and Mn contents significantly change at resonant frequencies [9, 12]. (3) When $V_c > V_{bCo}{}^{2+}$ or $V_{bMn}{}^{2+}$, the Co and Mn contents approach saturated values, respectively.

Figure 2 shows a typical diagram for Mn content, C_{Mn} under the condition $C_{Mn}+C_{co}=1$ assuming $V_{bMn}{}^{2+} > V_{bCo}{}^{2+}$. The slopes of the Mn content are slightly different at $V_c = V_{bCo}{}^{2+}$. This is because the Co content becomes constant at $V_c \geq V_{bCo}{}^{2+}$. The two arrows denote that oscillatory changes in the Mn content occur at resonant frequencies when $V_c = V_{bCo}{}^{2+}$ or $V_{bMn}{}^{2+}$. When $V_c > V_{bMn}{}^{2+}$, the Mn content tends to become constant.

3.2 Potential barriers of Co^{2+} and Mn^{2+}

Figure 3 shows the dependence of the Mn content of Co–Mn thin films on the cathode potentials at 0.4, 0.45, and 0.5 MHz. According to the phenomenological theory for the multi-component electrodeposition [9], the Mn content of the electrodeposits increases with V_c and tends to become constant irrespective of the frequencies. When $V_c = V_{bMn}{}^{2+}$ or $V_{bCo}{}^{2+}$, oscillatory changes in the Mn content occur at resonant frequencies. Figure 3 shows that the dependence of the Mn content on the cathode potential is similar to that of the Mn content in Fig. 2.

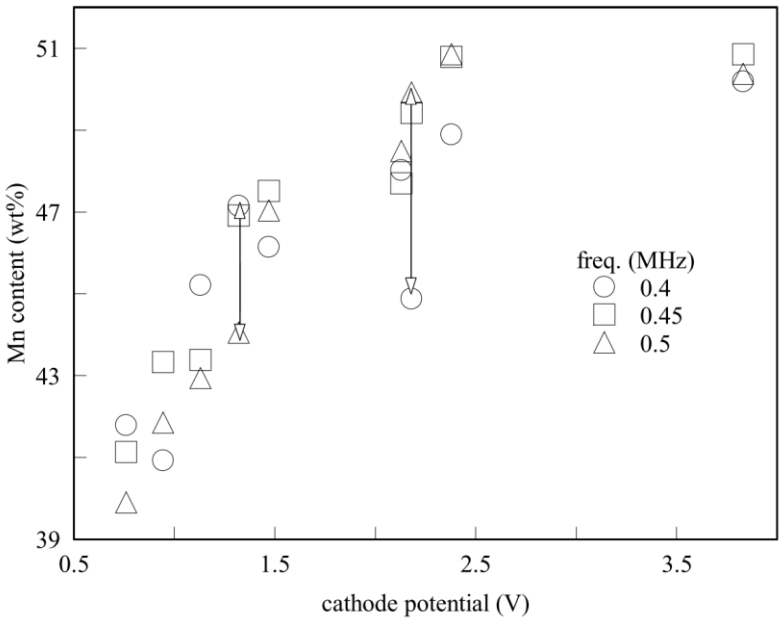

Figure 3. Dependence of the Mn content of Co–Mn thin films on the cathode potential. The arrows show large changes in the Mn content at $V_c = V_{bi}$ (i=Co^{2+} or Mn^{2+})

The two arrows in Fig. 3 denote the two large changes in the Mn content between 0.4 and 0.5 MHz. The potential barrier of Co^{2+} was determined to be 1.32 V because of the large change in the Mn content. The Mn^{2+} potential barrier was also determined to be 2.26 V because the Mn content significantly changed at V_c = 2.26 V and approached 50.3±1.4 wt% at V_c > 2.26 V.

3.3 Frequency-dependence of Co and Mn contents

Figure 4 shows the dependence of the Co content of Co–Mn thin films on the frequency at V_c=1.32 V, which is the potential barrier of Co^{2+} as determined from Fig. 3. In quaternary Co–Ni–Fe–Mn electrodeposition [9], the Co^{2+} potential barrier was 1.12 V. However, the factors affecting the potential barrier are not known yet. The Co content of the Co–Mn thin films changed in the range of 51.8–56.0 wt%. The Mn content had a local maximum at the resonant frequencies of 0.5, 0.65, 0.8, 0.9, 1.0, 1.05, 1.1, and 1.2 MHz. The mean resonant frequency spacing between the neighboring resonant frequencies was 0.108 MHz, which is approximately consistent with that observed for Co–Ni electrodeposition [12]. The mean local minimum of the Co contents at 0.4, 0.6, 0.85, 1.05, and 1.1 MHz is 52.4 wt%, which indicates that Co atoms were formed from Co^{2+} ions by the electron transition from the Fermi level to the upper state of Co^{2+}.

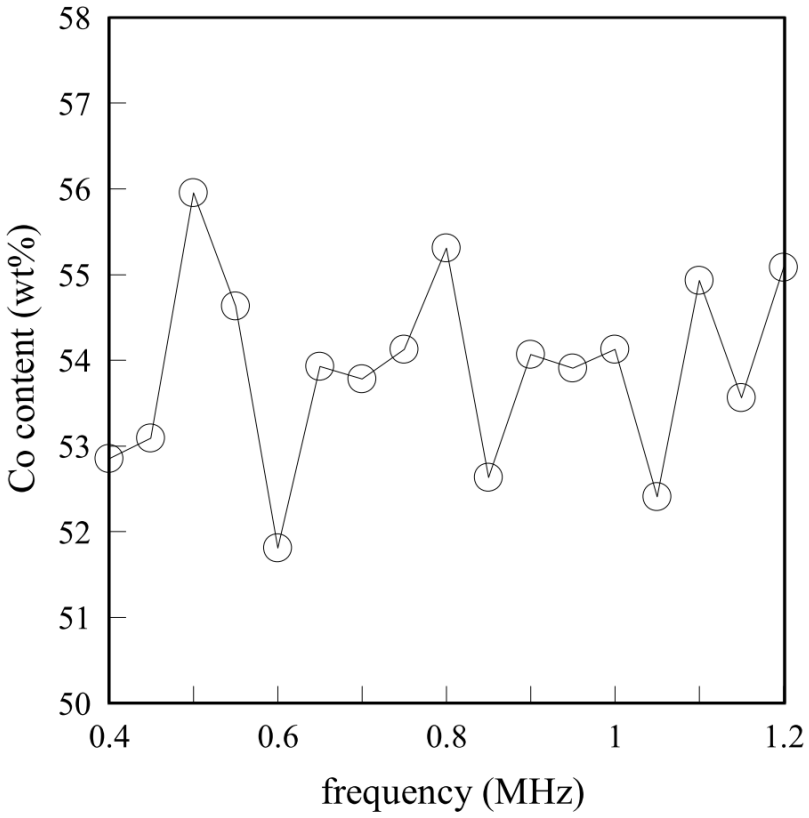

Figure 4. Frequency-dependence of the Co content of Co–Mn thin films electrodeposited at V_c=1.32 V.

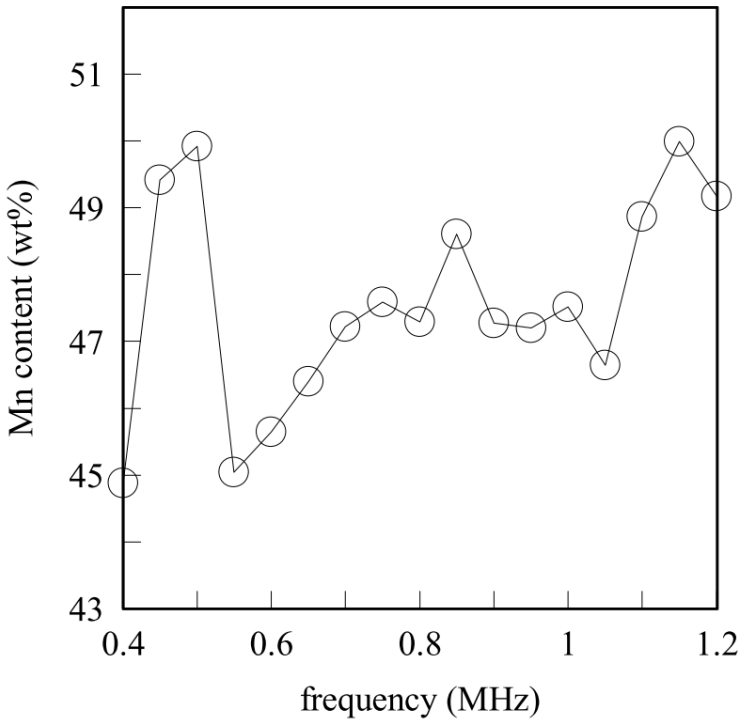

Figure 5. Frequency-dependence of the Mn content of Co–Mn thin films electrodeposited at V_c= 2.26 V.

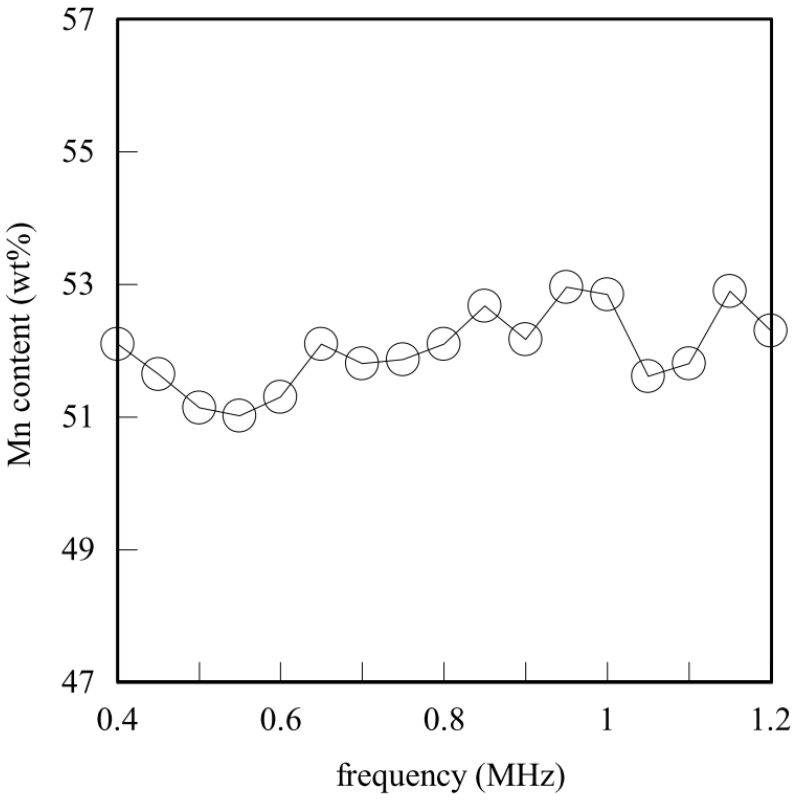

Figure 6. Frequency-dependence of the Mn content of Co–Mn thin films electrodeposited at V_c= 4.42 V.

Figure 5 shows the dependence of the Mn content of Co–Mn thin films on the frequency at V_c=2.26 V, which is the Mn^{2+} potential barrier. The Mn content oscillation occurred in the range of 44.8–50.0 wt% of Mn. The mean resonant frequency spacing between the neighboring resonant frequencies was 0.125 MHz. The Mn content at the resonant frequency of 0.5 MHz increased by 5 wt%. This indicates that 5 wt% of Mn was formed by electron transition from the Fermi level to the multi-quantized rotational energy level of Mn^{2+}.

Figure 6 shows the dependence of the Mn content of Co–Mn thin films on the frequency at V_c=4.42 V. The Mn content changed in the range of 51.0–52.9 wt%. In comparison with Figs. 4 and 5, Fig.6 shows smaller changes in the Mn content with frequencies. The variance of the Mn content in Fig. 6 resulted from the measured errors of EDX and the spatial distribution of Mn in Co–Mn thin films. As shown in Figs. 4 and 5, the change in the Mn content of the Co–Mn thin films at the resonant frequencies were large.

The mean Mn content of the Co–Mn thin films in Fig. 6 was 52.0 wt%, which was larger than the Mn content of 47.3 wt% in the solution. The activity of Mn^{2+} ions was apparently larger than the Mn content in the solution.

3.4 Crystalline structure of Co–Mn thin films

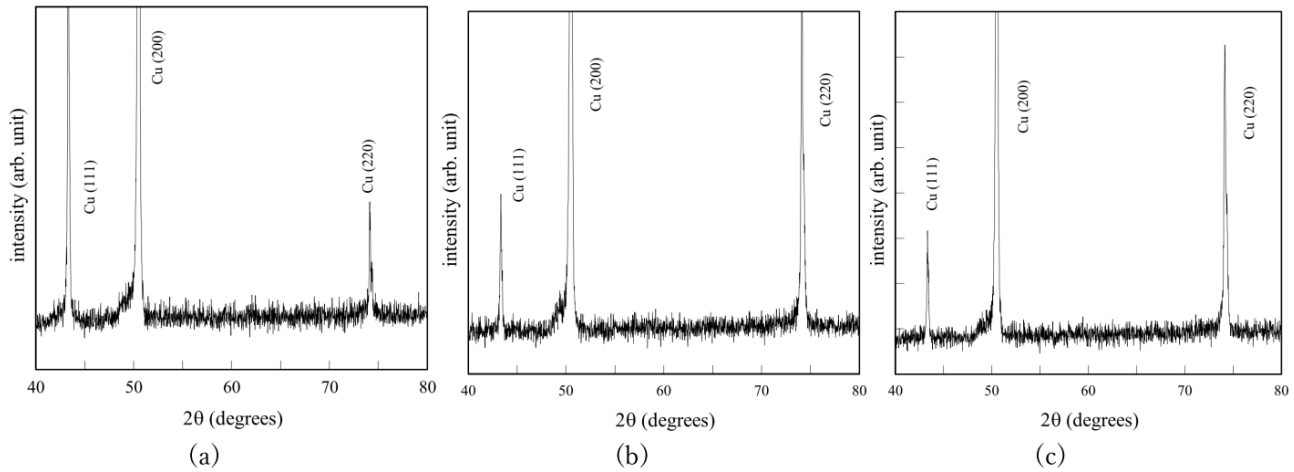

Figure 7. XRD charts of 2.3 μm Co–Mn thin films: (a) V_c= 1.32 V and 0.5 MHz, (b) V_c= 2.26 V and 1.15 MHz, and (c) V_c= 4.42 V and 0.95 MHz.

Figure 7 shows XRD charts of 2.3 μm thick Co–Mn thin films formed at the cathode potentials of 1.32, 2.26, and 4.42 V. The Mn contents of Co–Mn thin films in Figs. 7 (a), (b), and (c) are 44.0, 50.0, and 53.0 wt%, respectively. No diffraction peak from Co–Mn thin films was observed. According to the Co–Mn phase diagram [10], Co–Mn alloys have an HCP Co and β–Mn phase in the range of 44–50 wt% Mn, and β–Mn phase when the Mn content > 50 wt%. In contrast, the Co–Mn thin films in this study had an amorphous structure.

4. CONCLUSIONS

The Mn contents of Co–Mn thin films electrodeposited by a rectangular pulse voltage over a megahertz frequency range were consistent with the dependence of the Mn content on the cathode potential predicted by the phenomenological theory for multi-component electrodeposition. The EDX analyses revealed the potential barriers of Co^{2+} and Mn^{2+} as 1.32 and 2.26 V, respectively. The oscillatory Mn contents of Co–Mn thin films electrodeposited at $V_c = V_{bMn}{}^{2+}$ or $V_{bCo}{}^{2+}$ were demonstrated. The Co–Mn films in the range of 40–56 wt% Mn were produced from a Co^{2+}/Mn^{2+} solution of 1.2 mole ratio. The XRD analysis showed that the Co–Mn thin films had amorphous structures.

References

1. J. Wu, C. D. Johnson, R. S. Gemmen, and X. Liu, *J. Power Sources*, 189 (2009) 1106.
2. H. Zhang, J. Yuan, and M. Zhul, *Int. J. Electrochem. Sci.*, 12 (2017) 8368.
3. T. D. Hall, H.A. McCrabb, J. Wu, H. Zhang, X. Liu, and E. J. Taylor, *ECS Trans.*, 28 (2010) 197.
4. S. Chen, H. Chen, C. Li, M. Fan, C. Lv, G. Tian, and K. Shu, *J. Mater. Sci.*, 52 (2017) 6687.
5. B. Zhou, Y-W. Zhang, C-S. Liao, F-X. Cheng, C-H. Yana, L-Y. Chen, and S-Y. Wang, *Appl. Phys. Lett.*, 79 (2001) 1849.
6. K. Cysewska, G. Cempura, J. Karczewski, M. Łapiński, P. Jasiński, and S. Molin, *Mater. Lett.*, 258 (2020) 126759.
7. I. Kharmachi, L. Dhouibi, P. Berçot, and M. Rezrazi, *J. Mater. Environ. Sci.*, 6 (7) (2015) 1807.
8. A. Karpuz, H. Kockar, and M. Alper, *Appl. Surf. Sci.*, 358 (2015) 605.
9. M. Saitou, *Int. J. Electrochem. Sci.*, 15(2020) 6561
10. W. Huang, *CALPHAD.*, 13 (1989) 231.
11. R. H. Fowler and L. Nordheim, *Proc. R. Soc. Ser. A*, 119 (1928) 173.
12. M. Saitou, *Int. J. Electrochem. Sci.*, 13 (2018) 305.